

# Femtosecond Time-Resolved Optical and Raman Spectroscopy of Photoinduced Spin Crossover: Temporal Resolution of Low-to-High Spin Optical Switching

Amanda L. Smeigh,<sup>†</sup> Mark Creelman,<sup>‡</sup> Richard A. Mathies,<sup>‡</sup> and James K. McCusker<sup>\*,†</sup>

Department of Chemistry, Michigan State University, East Lansing, Michigan 48824, and the Department of Chemistry, University of California at Berkeley, Berkeley, California 94720

Received July 29, 2008; E-mail: jkm@chemistry.msu.edu

Understanding the mechanisms by which molecules interconvert among their distinct electronic and/or geometric configurations in response to external perturbations constitutes an important step toward the development of molecular-based materials.<sup>1</sup> Low-spin Fe<sup>II</sup> complexes comprise an intriguing class of compounds in this regard due to their potential utility in solar energy conversion strategies<sup>2</sup> as well as the basis for magneto-optical devices.<sup>3</sup> It is well-known that photoexcitation of such compounds results in the eventual formation of the high-spin form of the molecule; the net two-quantum spin conversion coincides with an exceptionally large structural reorganization ( $\Delta r_{\text{Fe-L}} \sim 0.2 \text{ \AA}$ ,  $\Delta V \sim 25 \text{ cm}^3 \text{ mol}^{-1}$ ), significant attenuation of the compound's optical density ( $\Delta\epsilon \sim 10^3 \text{ M}^{-1} \text{ cm}^{-1}$ ), and a dramatic change in the compound's magnetic properties ( $S = 0 \rightarrow S = 2$ ).<sup>4</sup> Several groups have exploited various spectroscopic probes in an effort to quantify the dynamics of this spin-state conversion but thus far have only been able to define an upper limit for the time constant associated with formation of the high-spin state.<sup>5</sup> In this report, we present femtosecond optical and stimulated Raman scattering data on a prototypical low-spin Fe<sup>II</sup> charge-transfer complex that, for the first time, kinetically resolves the formation of the high-spin state and thus defines the time scale for optical switching in this class of compounds.

The compound under study is  $[\text{Fe}(\text{tren}(6\text{-R-py})_3)]^{2+}$  (R = H (1), CH<sub>3</sub> (2)), which is illustrated in Chart 1 along with a simplified energy level diagram showing the low-lying ligand-field excited states of a d<sup>6</sup> transition metal ion. As shown by Drago and co-workers,<sup>6</sup> this compound sits very close to the so-called spin-crossover point wherein the energies of the low-spin (<sup>1</sup>A<sub>1</sub>) and high-spin (<sup>5</sup>T<sub>2</sub>) forms are in close proximity. Compound 1 possesses a low-spin ground state, whereas the steric constraints imposed by the introduction of the CH<sub>3</sub> groups in compound 2 require an elongation of the Fe–N bond, resulting in stabilization of the high-spin <sup>5</sup>T<sub>2</sub> term as its ground state. This system thus has the unique characteristic of having reciprocal ground- and lowest-energy excited states; i.e., the lowest-energy excited state of one corresponds to the ground state of the other. We have previously exploited this feature to probe the ultrafast electronic absorption spectroscopy of  $[\text{Fe}(\text{tren}(\text{py})_3)]^{2+}$  in the visible region and have shown that charge-transfer excitation of this compound results in the formation of the <sup>5</sup>T<sub>2</sub> state in <1 ps.<sup>5a</sup>

Owing to the nature of the absorption spectra of the low-spin and high-spin forms of the molecule, more diagnostic features can be found in the ultraviolet region of the spectrum. Specifically, there exist two isosbestic points between the <sup>1</sup>A<sub>1</sub> and <sup>5</sup>T<sub>2</sub> states at  $285 \pm 5 \text{ nm}$  and  $320 \pm 5 \text{ nm}$  as indicated by the calculated differential absorption spectrum between compounds 1 and 2 as well as data

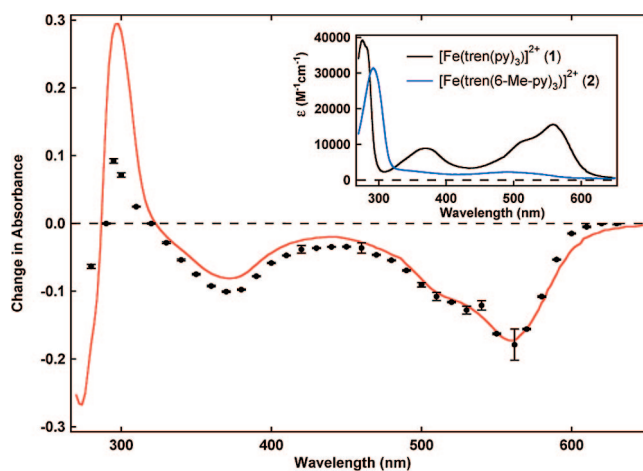
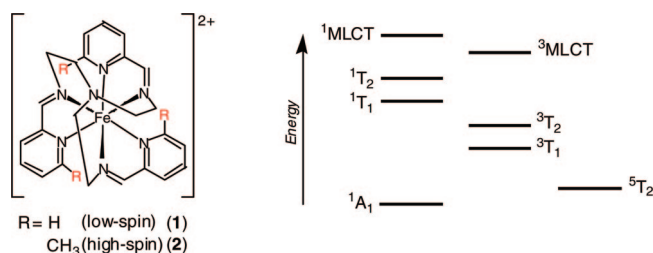


**Figure 1.** Differential absorption spectra for  $[\text{Fe}(\text{tren}(6\text{-R-py})_3)](\text{PF}_6)_2$  in  $\text{CH}_3\text{CN}$  solution. The data points correspond to amplitudes from fits of nanosecond time-resolved absorption data acquired following <sup>1</sup>A<sub>1</sub> → <sup>1</sup>MLCT excitation of compound 1 (R = H) at 560 nm, whereas the solid red line is a difference spectrum calculated from the ground-state absorption spectra of compounds 1 and 2 (inset). Wavelengths for which the change in absorbance is zero correspond to isosbestic points between the <sup>1</sup>A<sub>1</sub> and <sup>5</sup>T<sub>2</sub> electronic states of this system.

**Chart 1.** Drawing of  $[\text{Fe}(\text{tren}(6\text{-R-py})_3)]^{2+}$  (Left), Along with a Qualitative Jablonski Diagram for Compound 1 Showing the Charge-Transfer and Low-Lying Ligand-Field States (Right)



from nanosecond time-resolved absorption spectroscopy (Figure 1).<sup>7</sup> These observations constitute important optical markers for establishing the formation of the <sup>5</sup>T<sub>2</sub> excited state of compound 1 following photoexcitation, since it is highly unlikely that three (or more) electronic states of a given molecule will simultaneously possess two coincident isosbestic points.

Accordingly, we have acquired femtosecond time-resolved differential absorption data in the ultraviolet region in order to determine at what point in time the low-spin/high-spin isosbestic of compound 1 are established. Measurements were carried out at probe wavelengths on both sides of the two isosbestic points and are shown in Figure 2.<sup>7</sup> The data at earliest times are complicated by the presence of features associated with the initially formed

<sup>†</sup> Michigan State University.  
<sup>‡</sup> University of California at Berkeley.

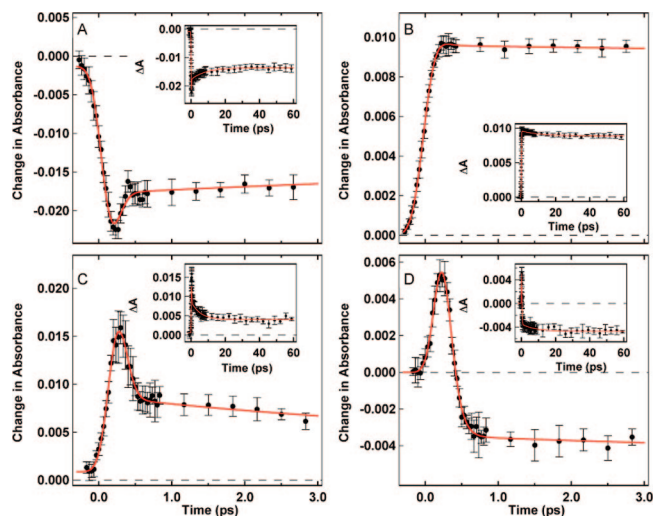


**Figure 2.** Femtosecond time-resolved differential absorption data for  $[\text{Fe}(\text{tren}(\text{py})_3)](\text{PF}_6)_2$  (**1**) in  $\text{CH}_3\text{CN}$  solution. Data were acquired at 285 (A), 290 (B), 315 (C), and 325 nm (D) following  $^1\text{A}_1 \rightarrow ^1\text{MLCT}$  excitation at 560 nm. The solid lines correspond to fits derived from a convolution of the instrumental response function with a biexponential kinetic model ( $\tau_1 < 250$  fs and  $\tau_2 = 5.5 \pm 1.5$  ps). See text for further details.

metal-to-ligand charge-transfer excited state. Previous work has demonstrated that the lifetime of the charge-transfer manifold of this system is ca. 100 fs.<sup>5a</sup> The rise and rapid decay in absorbance that is evident at 315 and 325 nm as well as the partial recovery of the signal at 285 nm can thus be attributed to this charge-transfer excited state based on their temporal profile<sup>5a</sup> in conjunction with spectroelectrochemical data obtained for compound **1** (Figure S1).

Notwithstanding these charge-transfer features, the data clearly show changes in the sign of the transient absorption signals at either side of the isosbestic points noted in Figure 1. Specifically, the net loss of absorbance at 285 nm coupled with the positive signal observed at 290 nm indicates that a zero-crossing (i.e., a point at which  $\Delta A = 0$ ) must occur between these two wavelengths. Similarly, a ground-state/excited-state isosbestic also exists between 315 and 325 nm. These spectral ranges coincide precisely with the low-spin/high-spin isosbestic points anticipated for  $[\text{Fe}(\text{tren}(\text{py})_3)]^{2+}$ . Our cross-correlation pulse width of 250 fs prohibits an accurate assessment of the kinetics, but the simultaneous presence of both sign changes anticipated from the calculated and nanosecond differential absorption spectra for  $[\text{Fe}(\text{tren}(\text{py})_3)]^{2+}$  provides compelling evidence that the  $^5\text{T}_2$  state for this molecule is formed in  $\tau < 250$  fs.

The actual time constant for high-spin formation was obtained from femtosecond stimulated Raman scattering (FSRS) experiments.<sup>7,8</sup> Analysis of the data was facilitated by comparing the time-resolved spectra with steady-state resonance Raman data acquired for both the low-spin parent compound **1** and its high-spin analogue, compound **2**; the latter provided an important benchmark for correlating the time-resolved data with the identity of the electronic state from which it originated. The steady-state and time-resolved spectra are plotted in Figure 3; kinetic traces corresponding to both spectral position and amplitude are shown in Figure 4. The most diagnostic region of the spectrum lies above  $1600 \text{ cm}^{-1}$ : the highest energy band, assigned to the Schiff base C=N stretch of the ligand, undergoes a hypsochromic shift of ca.  $33 \text{ cm}^{-1}$  between the low-spin and high-spin forms. This is consistent with the attenuation of  $\pi$ -backbonding expected following conversion from the (nominally)  $t_{2g}^6$  electronic configuration associated with the  $^1\text{A}_1$  state to the  $t_{2g}^4 e_g^2$  configuration of the high-spin species.

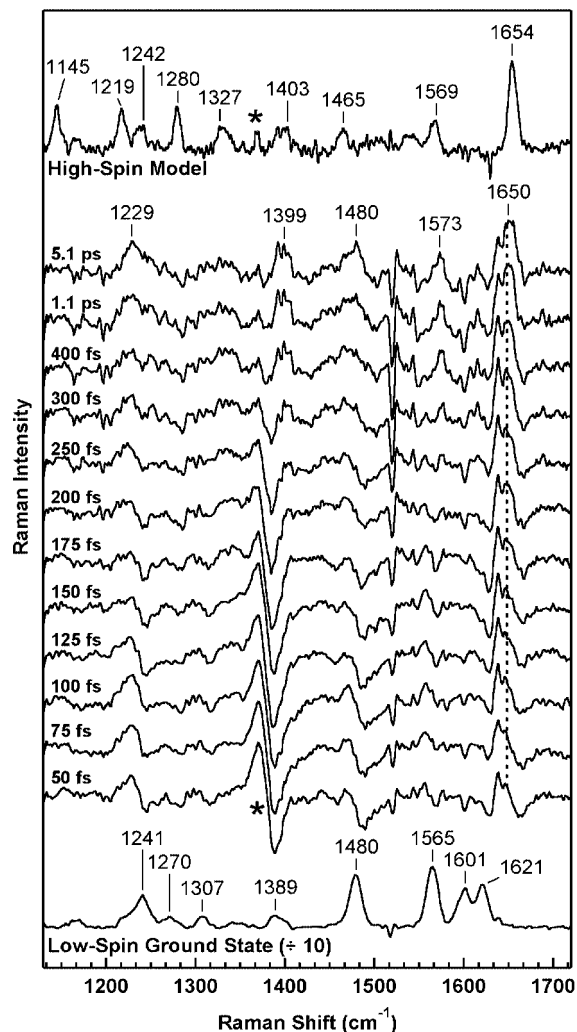


**Figure 3.** Femtosecond stimulated Raman scattering spectra for  $[\text{Fe}(\text{tren}(\text{py})_3)](\text{PF}_6)_2$  (**1**) in  $\text{CH}_3\text{CN}$  solution. Electronic excitation was carried out at 560 nm with a Raman pump pulse centered at 792 nm. Steady-state Raman spectra for compounds **1** and **2** are shown at the bottom and top of the figure, respectively; inset numbers to the left of the stacked spectra correspond to delay times of the Raman pump relative to the excitation pulse. The dispersive feature at  $1376 \text{ cm}^{-1}$  (indicated by \*) is due to the solvent. Additional experimental details can be found in the Supporting Information.

Excitation into the  $^1\text{MLCT}$  excited state results in a formal oxidation of the metal center to  $\text{Fe}^{\text{III}}$  and reduction of the pyridyl ring(s): the appearance of the C=N stretch to the blue side of the ground-state value of  $1621 \text{ cm}^{-1}$  at  $\Delta t = 50$  fs therefore likely reflects this photoinduced shift in charge density, as does the slight red shift of the pyridyl ring C=C and/or C=N stretch(es) at  $1460 \text{ cm}^{-1}$ .<sup>9</sup> As the spectrum evolves, a feature near  $1650 \text{ cm}^{-1}$  characterized by a progression to higher energy develops during the first ca. 500 fs followed by a more gradual change on a longer (i.e., picosecond) time scale. The shift in the maximum of this band can be accurately described using a biphasic exponential model with time constants  $\tau_1 = 190 \pm 50$  fs and  $\tau_2 = 10 \pm 3$  ps (Figure 4A). Given that the electronic evolution of the compound is complete in  $< 250$  fs (Figure 2),  $\tau_2$  can be confidently assigned to vibrational relaxation within the  $^5\text{T}_2$  ligand-field state. The value is within experimental error of the second kinetic component used to model the data in Figure 2 as well as our previous observations from electronic absorption spectroscopy on compound **1**.<sup>5a</sup> Similar conclusions have been drawn from femtosecond time-resolved

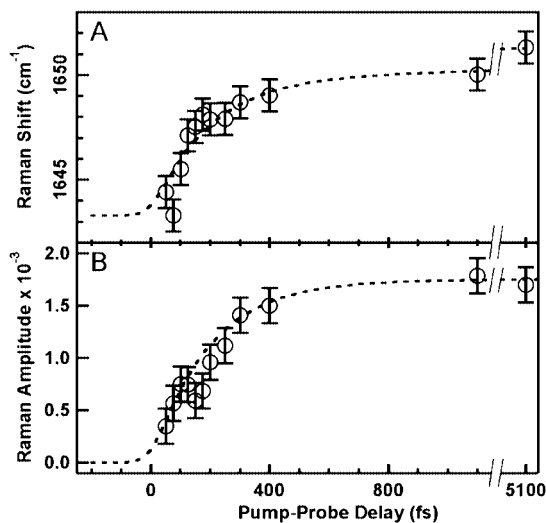


**Figure 4.** Time dependence of the change in energy (A) and spectral amplitude (B) of the C=N stretching vibration of [Fe(tren(py)<sub>3</sub>)](PF<sub>6</sub>)<sub>2</sub> (**1**) derived from the femtosecond stimulated Raman scattering data shown in Figure 3. The dashed lines correspond to fits to exponential kinetic models. Both the spectral shift and amplitude can be modeled with the same initial time constant  $\tau = 190 \pm 50$  fs; the spectral shift exhibits a second component with  $\tau_2 = 10 \pm 3$  ps. See text for further details.

infrared data on other systems, reflecting an emerging consensus on the approximate time scale for vibrational relaxation in coordination compounds.<sup>10</sup>

The fact that the formation of both isosbestic points occurs on a time scale similar to  $\tau_1$  suggests that these kinetics are diagnostic of the structural evolution associated with the low-to-high spin conversion;<sup>11</sup> the time-dependent shift of the C=N stretching frequency to higher energy reflects the aforementioned reduction in metal–ligand back-bonding that is expected to occur concomitant with the formation of the <sup>5</sup>T<sub>2</sub> state. This assignment is further supported by the temporal profile of the Raman amplitude (Figure 4B). Specifically, the increase in amplitude, which exhibits kinetics identical to the spectral shift described by  $\tau_1$ , indicates an increase in the polarizability of the chromophore. This is consistent with a low-to-high spin conversion due to the larger molecular volume and smaller metal–ligand force constants associated with the <sup>5</sup>T<sub>2</sub> state. The lack of a second component in the time–amplitude trace is likewise consistent with this picture given that vibrational cooling is occurring on the <sup>5</sup>T<sub>2</sub> surface, i.e., subsequent to the major electronic and structural changes of the system.

The results presented herein have several important implications. First, from a fundamental perspective, the fact that a net  $\Delta S = 2$  conversion has been quantified with a rate constant of ca.  $5 \times 10^{12}$  s<sup>-1</sup> raises interesting questions in terms of the applicability of

existing theoretical formalisms for describing nonradiative decay dynamics in molecular systems.<sup>5d</sup> Second, the formation of low-lying ligand-field states has been implicated as an important decay pathway limiting the utility of transition metal-based chromophores in certain solar energy conversion strategies;<sup>5a,b</sup> the data we have obtained serve to define an important kinetic benchmark in this regard. Lastly, the applicability of spin-crossover systems to optical device development relies in part on rapid, efficient photoinduced interconversion between the low-spin and high-spin states.<sup>3</sup> Our results suggest that switching times for devices employing such compounds could be extremely rapid. Efforts to probe these questions as well as assess the generality of the results we have presented are ongoing.

**Acknowledgment.** This work was supported by the Chemical Sciences, Geosciences, and Biosciences Division, Office of Basic Energy Sciences, U.S. Department of Energy Grant No. DE-FG02-01ER15282 (J.K.M.), and the Mathies Royalty Fund (R.A.M.).

**Supporting Information Available:** Plots of spectroelectrochemical data for [Fe(tren(py)<sub>3</sub>)](PF<sub>6</sub>)<sub>2</sub> in CH<sub>3</sub>CN solution (Figure S1); sample analysis of femtosecond stimulated Raman spectra (Figure S2); description of experimental procedures. This material is available free of charge via the Internet at <http://pubs.acs.org>.

## References

- (1) (a) Balzani, V.; Credi, A.; Venturi, M. *Nano Today* **2007**, *2*, 18, and references therein. (b) Kay, E. R.; Leigh, D. A.; Zerbetto, F. *Angew. Chem., Int. Ed.* **2007**, *46*, 72 and references therein.
- (2) Ferrere, S.; Gregg, B. A. *J. Am. Chem. Soc.* **1998**, *120*, 843. For a more general discussion, see: Meyer, G. *Inorg. Chem.* **2005**, *44*, 6852.
- (3) Letard, J. F. *J. Mater. Chem.* **2006**, *16*, 2550, and references therein.
- (4) Gutlich, P.; Goodwin, H. A., Eds. *Spin Crossover in Transition Metal Compounds. Topics in Current Chemistry*; Springer: Berlin, 2004; Vols. 233–235.
- (5) (a) Monat, J. E.; McCusker, J. K. *J. Am. Chem. Soc.* **2000**, *122*, 4092. (b) Juban, E. A.; Smeigh, A. L.; Monat, J. E.; McCusker, J. K. *Coord. Chem. Rev.* **2006**, *250*, 1783. (c) Wolf, M. M. N.; Groß, R.; Schumann, C.; Wolny, J. A.; Schünemann, V.; Dössing, A.; Paulson, H.; McGarvey, J. J.; Diller, R. *Phys. Chem. Chem. Phys.* **2008**, *10*, 4264. (d) Gawelda, W.; Cannizzo, A.; Pham, V. T.; van Mourik, F.; Bressler, C.; Chergui, M. *J. Am. Chem. Soc.* **2007**, *129*, 8199.
- (6) Hoselton, M. A.; Wilson, L. J.; Drago, R. S. *J. Am. Chem. Soc.* **1975**, *97*, 1722.
- (7) Experimental details can be found in the Supporting Information.
- (8) Kukura, P.; McCamant, D. W.; Mathies, R. A. *Annu. Rev. Phys. Chem.* **2007**, *58*, 461.
- (9) The presence of the CH<sub>3</sub> group in compound **2** is expected to shift the pyridyl ring vibrations in the ca. 1450–1550 cm<sup>-1</sup> region to somewhat lower energies relative to compound **1**.
- (10) For recent examples, see: (a) Henry, W.; Coates, C. G.; Brady, C.; Ronayne, K. L.; Matousek, P.; Towrie, M.; Botchway, S. W.; Parker, A. W.; Vos, J. G.; Browne, W. R.; McGarvey, J. J. *J. Phys. Chem. A* **2008**, *112*, 4537. (b) Maçõas, E. M. S.; Kananavicius, R.; Myllyperkiö, P.; Pettersson, M.; Kunttu, H. *J. Am. Chem. Soc.* **2007**, *129*, 8934. (c) Juban, E. A.; McCusker, J. K. *J. Am. Chem. Soc.* **2005**, *127*, 6857.
- (11) A relaxation pathway of <sup>1</sup>MLCT → <sup>3</sup>MLCT → <sup>5</sup>T<sub>2</sub> has been identified for [Fe(bpy)<sub>3</sub>]<sup>2+</sup> (cf. 5d). In the present case, only a single process (i.e.,  $\tau_1$ ) reflecting the overall conversion to the <sup>5</sup>T<sub>2</sub> state was resolved.

JA805949S